ANOMALOUS DIFFUSION

ANJA PIRNAT

Fakulteta za matematiko in fiziko
Univerza v Ljubljani

Many processes in nature have been observed to deviate from normal diffusion. Their mean squared displacement grows either sublinearly or superlinearly in time. Such phenomena is called anomalous diffusion. As a model of ordinary diffusion random walk is presented. Then the generalization to continuous time random walk is made. In this model long waiting times and long jumps can be included and thus make a continuous time random walk suitable model to describe anomalous diffusion. Lastly, two examples of anomalous: sub- and super-diffusion are presented.

ANOMALNA DIFUZIJA

V naravi je mnogo procesov, ki niso v skladu z normalno difuzijo, njihov kvadrat oddaljenosti s časom raste bodisi sublinearno ali superlinearno, kar je značilno za anomalno difuzijo. V članku je kot model normalne difuzije predstavljen model naključnega sprehoda. Sledi predstavitev časovno zveznega naključnega sprehoda, ki omogoča vključitev dolgih korakov in dolgih čakalnih časov. Ta model dobro opiše nekatere procese anomalne difuzije. Na koncu članka sta predstavljena tudi dva primera anomalne difuzije; en subdifuzijski in en superdifuzijski.

1. Introduction

The first phenomenological description of diffusion was done by Fick in 1855 after studying transport trough membranes in living organisms. He assumed that to reach equilibrium particles have to flow against the concentration gradient. Combining this assumption with the continuity equation he obtained diffusion equation for the evolution of particles' concentration $c(x, t)$,

$$\frac{\partial}{\partial t}c(x,\,t) = K\frac{\partial^2}{\partial x^2}c(x,\,t), \tag{1}$$

where K denotes the diffusion coefficient (we have written the equation for one dimension). The same equation holds for probability density function (abbreviated by PDF) $p(x,\,t)$ to find a particle at position x at time t. For an ensemble of particles starting at the origin $x = 0$ its evolution is given by Gaussian function with variance $2Kt$. Mean square displacement (abbreviated by MSD) of the particles is then easily calculated by

$$\left\langle x^2(t) \right\rangle = \int_{-\infty}^{+\infty} x^2 p(x,\,t)\mathrm{d}x = 2Kt. \tag{2}$$

We see that MSD scales linearly with time, which is characteristic of normal diffusion described by Eq. (1). Fifty years after Fick's derivation notable work on diffusion was done by Einstein who studied Brownian motion based on microscopic principles. Using statistical mechanics he obtained same expression for MSD as in Eq. (2), moreover, he was able to relate K to measurable physical quantities.

In the following years many processes have been observed that deviated from the normal diffusion; from the movement of charges in amorphous semiconductors [1], to flight of an albatross [2], for a brief overview see Refs. [3], [4]. Such processes are described by anomalous diffusion for which MSD scales as power law

$$\left\langle x^2(t) \right\rangle \simeq K_\alpha t^\alpha \tag{3}$$

where K_α is a generalized diffusion coefficient with physical dimension $\mathrm{m}^2\mathrm{s}^{-\alpha}$. Systems with $0 < \alpha < 1$ display subdiffusion, meaning that the transport is slower than the normal diffusion, while values of $\alpha > 1$ correspond to superdiffusion.
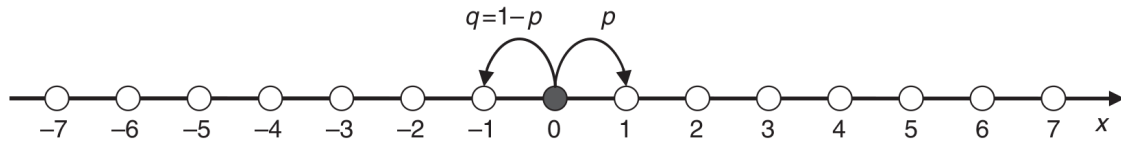
Slika 1. Schematic depiction of a one-dimensional random walk on a periodic lattice. Reproduced from [5].

In the article we will first use a simple random walk model to derive the diffusion equation and corresponding MSD. In the following chapter continuous time random walk (abbreviated by CTRW) model will be presented as the generalization of a random walk. We will show that heavy-tailed PDFs without finite moments lead to anomalous diffusion. Lastly, two examples that can be accurately modeled with the CTRW approach will be presented.

2. Random Walk

2.1 Derivation of the Diffusion Equation

To derive the diffusion equation in one dimension we start with a simple random walk on a one-dimensional periodic lattice. In discrete time steps particle can either jump to the right $(j \to j+1)$ with probability p or to the left $(j \to j-1)$ with probability $q = 1 - p$, see Fig. 1. We consider the case of a symmetric random walk, $p = q = \frac{1}{2}$. Let $P_n(j)$ denote the probability that particle is at site j after performing n steps. The illustrated process can be modeled by the evolution equation

$$P_{n+1}(j) = \frac{1}{2}P_n(j-1) + \frac{1}{2}P_n(j+1). \tag{4}$$

In order to pass to a continuum limit, we first replace the discrete variables (j, n) by continuous variables (x, t). The relations between pairs of variables are $x = j\Delta x$ and $t = n\Delta t$, where Δx is the lattice constant and Δt is the time span between two successive steps. Then we let both Δx and Δt approach zero so that we can expand Eq. (4) in a Taylor series around $\Delta x = \Delta t = 0$. The lowest orders in the required expansion are

$$P(j\Delta x,\, [n+1]\Delta t) = P(x,\, t) + \Delta t \frac{\partial P(x,\, t)}{\partial t} + O(\Delta t^2), \tag{5}$$

$$P([j \pm 1]\Delta x,\, n\Delta t) = P(x,\, t) \pm \Delta x \frac{\partial P(x,\, t)}{\partial x} + \frac{1}{2}\Delta x^2 \frac{\partial^2 P(x,\, t)}{\partial x^2} + O(\Delta x^3). \tag{6}$$

Substituting these expressions in Eq. (4) and retaining the lowest orders in Δt and Δx leads to the diffusion equation

$$\frac{\partial P(x,\, t)}{\partial t} = K \frac{\partial^2 P(x,\, t)}{\partial x^2}. \tag{7}$$

Note that the continuum limit has to be drawn such that the quotient

$$K \equiv \lim_{\Delta t, \Delta x \to 0} \frac{\Delta x^2}{2\Delta t} \tag{8}$$

is finite. K denotes the diffusion coefficient and is of dimension $[K] = \mathrm{m}^2\mathrm{s}^{-1}$. For more detailed derivation see Ref. [6].

2.2 Mean Squared Displacement

In this section we discuss how the MSD (2) emerges from the simple random walk model depicted in Sec. 2.1. Let Δx_1, Δx_2, ..., Δx_n be the displacements of test particle in the 1st, 2nd, ..., n-th step. Then the position of the particle after n steps is given by the sum of single-step displacements

$$x_n = \sum_{i=1}^{n} \Delta x_i. \tag{9}$$

The MSD of a particle after n steps is given in terms of jump-jump correlation function $\langle \Delta x_i \Delta x_k \rangle$,

$$\left\langle x_n^2 \right\rangle = \left\langle \left(\sum_{i=1}^{n} \Delta x_i \right)^2 \right\rangle = \sum_{i,\,k=1}^{n} \langle \Delta x_i \Delta x_k \rangle = \sum_{i=1}^{n} \langle \Delta x_i^2 \rangle + \sum_{i \neq k \,\wedge\, i,\,k \in \{1,\,n\}} \langle \Delta x_i \Delta x_k \rangle. \tag{10}$$

Since the jumps are assumed to be independent with zero average and thus uncorrelated the last term in the Eq. (10) vanishes. As the MSD of one jump is $\langle \Delta x_i^2 \rangle = \Delta x^2$ and it takes Δt to complete each step we obtain the following expression for MSD,

$$\left\langle x_n^2 \right\rangle = n\Delta x^2 = \frac{\Delta x^2}{\Delta t} t. \tag{11}$$

Comparing the Eq. (11) and definition of diffusion coefficient (8) we can rewrite MSD in the form $\left\langle x_n^2 \right\rangle = 2Kt$, which is exactly the known MSD expression (2) [7].

3. Continuous Time Random Walk

The continuous time random walk model can be viewed as a direct generalization of the random walk described in Chapter 2. Consider a particle starting at the origin $x = 0$. Before it makes an instantaneous jump to the left or right it waits a random time τ drawn from the waiting time PDF $\psi(\tau)$. The length of the jump l can also be chosen to be a random variable, distributed according to PDF $w(l)$. After the jump, a new pair of waiting time and jump length is drawn from the PDFs $\psi(\tau)$ and $w(l)$. The described model will be considered under the assumption that the new pairs of τ and l are fully independent of their previous values. Moreover, we will assume unbiased CTRW process, meaning that the jump length distribution is symmetric, $w(-l) = w(l)$ such that $\langle l \rangle = 0$ [8].

With these definitions a CTRW can be described with the recursion integral equation [9]

$$p(x,\,t) = \delta(x)\Psi(t) + \int_0^t \psi(t - t') \left[\int_{-\infty}^{+\infty} w(x - x')p(x',\,t')\mathrm{d}x' \right] \mathrm{d}t', \tag{12}$$

which relates the PDF $p(x,\,t)$ of particle being at position x at time t with an event of being at point x' at instant t', $p(x',\,t')$. $\Psi(t) = \int_t^{\infty} \psi(\tau)\mathrm{d}\tau$ denotes the survival probability that at time t particle is still at the origin $x = 0$. For many purposes the integral equation (12) can be easily treated by using Fourier and Laplace transforms, see Refs. [5], [9], [10]. However, in this article we will restrain from any long derivations and in the following only state the results.

Different types of CTRW processes can be categorized by the characteristic waiting time

$$\langle \tau \rangle = \int_0^{\infty} \tau \psi(\tau) \mathrm{d}\tau \tag{13}$$

and second moment of jump length PDF $w(l)$

$$\langle l^2 \rangle = \int_{-\infty}^{+\infty} l^2 w(l) \mathrm{d}l \tag{14}$$

being finite or diverging, respectively. The main input is therefore the form of PDFs $\psi(\tau)$ and $w(l)$.

Let us first study both moments $\langle\tau\rangle$ and $\langle l^2\rangle$ being finite. In the limit of large number of jumps this type of CTRW corresponds to Brownian motion with MSD (2), where the diffusion coefficient is defined as $K = \langle l^2\rangle/2\langle\tau\rangle$. Apart from moments affecting the value of K, the details of PDFs $\psi(\tau)$ and $w(l)$ are irrelevant for the normal diffusive process [8]. This is a direct consequence of central limit theorem stating that properly normed sum of a set of random variables, each with finite variance, will tend toward a Gaussian distribution as the number of summands increases [5].

If $\psi(\tau)$ and $w(l)$ are heavy-tailed distributions the moments diverge and thus give rise to anomalous behavior. In other words, as the heavy-tailed distributions have exponentially unbound tails, some extremely large waiting periods or jumps will occur and dominate the particle's behavior. See Fig. 2 for comparison of CTRWs of exponential waiting time PDF with finite moment $\langle\tau\rangle$ and heavy-tailed power-law distribution with diverging $\langle\tau\rangle$. We can observe that in the case of heavy-tailed PDF jumps happen quite irregularly, also when the time progresses probability for longer rests increases.

(a)

(b)
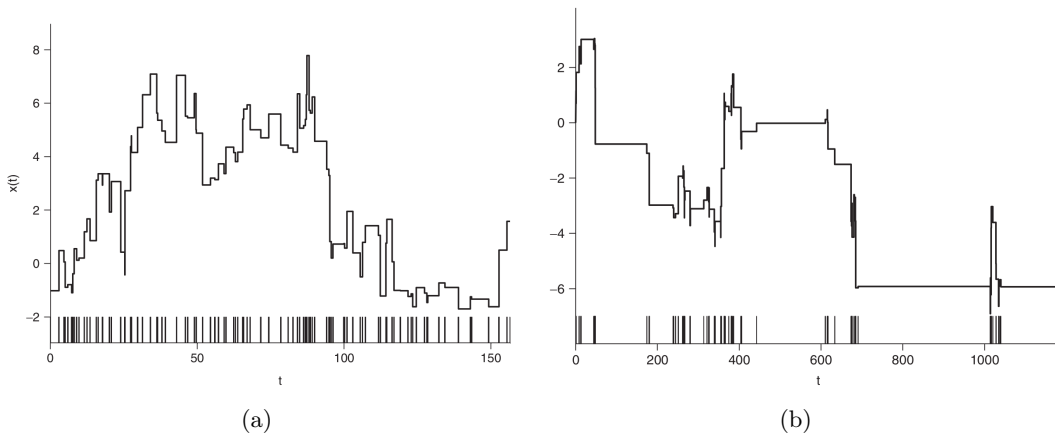
Slika 2. Trajectories of a CTRW with a Gaussian distribution of step length and exponential distribution of waiting times, $\psi(\tau) = e^{-t}$, in case (a) and power-law distribution of waiting times, $\psi(\tau) \sim t^{-3/2}$, in case (b). Barcode-like pattern at the bottom represents events of jumps. Reproduced from [5].

3.1 Subdiffusive Continuous Time Random Walk

We assume that jump lengths are sufficiently narrowly distributed such that $\langle l^2\rangle$ is finite and the waiting times are drawn from PDF that behaves asymptotically ($\tau \to \infty$) as power law

$$\psi(\tau) \sim \frac{\tau_0^\alpha}{\tau^{1+\alpha}}, \quad 0 < \alpha < 1, \tag{15}$$

in which the constant τ_0 is a scaling factor corresponding to some fundamental time scale of the process [8]. In Eq. (15) the lover bound ($0 < \alpha$) assures $\psi(\tau)$ to be normalized, while the upper bound corresponds to finite $\langle\tau\rangle$. Such waiting time distribution leads to anomalous behavior with MSD:

$$\langle x(t)^2\rangle \simeq K_\alpha t^\alpha, \tag{16}$$

where the generalized diffusion coefficient is defined as $K_\alpha = \frac{\langle l^2\rangle}{\tau_0^\alpha}$ [10].

To derive MSD (16) from waiting time PDF (15) in exact manner we would first have to Laplace transform $\psi(\tau)$ and then perform further calculations in Fourier-Laplace space using transformed

expression for particle's PDF (12). As such approach is out of scope for this article, we will only present a simple example to illustrate how MSD scaling can be estimated from waiting time PDF. We have a heavy-tailed waiting time PDF ($\alpha = 1/2$) of the form

$$\psi(\tau) \sim \frac{\exp\left(-a/\tau\right)}{\tau^{3/2}}, \tag{17}$$

where a is some positive constant. Waiting time distribution with same asymptotic behavior, $\sim \tau^{-3/2}$, is shown in the Fig. 2(b). $\psi(\tau)$ (17) is a Lévy stable distribution, meaning that it preserves its shape under convolution. PDF $\phi_n(t)$ to make n steps up to time $t = \tau_1 + \tau_2 + ... + \tau_n$ is given in the form of convolution

$$\phi_n(t) = \int_0^\infty \phi_{n-1}(t')\psi(t-t')\mathrm{d}t', \tag{18}$$

where $\phi_{n-1}(t')$ denotes the probability to make $n-1$ steps up to time t'. Since $\psi(\tau)$ (17) is a stable distribution, generalized central limit theorem can be applied [11]. For our selection of $\psi(\tau)$ (17) this means, that in the limit of $n \to \infty$ rescaled sum of n waiting times, $\frac{t}{n^2}$, tends to Levy stable distribution independent of n and of the same form as $\psi(\tau)$. From this we can deduce that the time in which n steps are preformed grows with n^2; number of steps up to time t scales as $n(t) \sim t^{1/2}$. MSD can be calculated as $\langle x^2(t) \rangle = \langle l^2 \rangle \langle n(t) \rangle$, where $\langle n(t) \rangle$ is a mean value of number of steps n up to time t. On approximating $\langle n(t) \rangle$ with $n(t)$ we get

$$\langle x^2(t) \rangle \sim t^{1/2}, \tag{19}$$

which is in agreement with Eq. (16).

3.2 Lévy Flight

We study a case with finite waiting time $\langle \tau \rangle$ and jump lengths being distributed symmetrically in terms of the asymptotic power-law PDF

$$w(l) \sim \frac{l_0^\mu}{|l|^{1+\mu}}, \quad 0 < \mu < 2, \tag{20}$$

in which l_0 is a scaling factor. In Eq. (20) upper bound ($\mu = 2$) corresponds to the finite $\langle l^2 \rangle$. Unlike in the case of subdiffusion, here the model solutions cannot be characterized by the second moment. Since the $\langle l^2 \rangle$ is infinite also the distribution of particle's final position has infinite MSD. However, for $\beta < \mu$ fractional moment can be calculated [10],

$$\left\langle |x(t)|^\beta \right\rangle = 2 \int_0^\infty x^\beta p(x,t)\mathrm{d}x \simeq (K_\mu t)^{\beta/\mu}, \tag{21}$$

where $K_\mu = l_0^\mu / \langle \tau \rangle$. PDF $p(x,t)$ in the above equation is obtained by first inserting Laplace transform of waiting time PDF and Fourier transform of jump lengths PDF (20) in Fourier- Laplace transformed Eq. (12) and then transforming it back to the (x,t) space. If we rescale fractional moment (21) according to

$$\left\langle |x(t)|^\beta \right\rangle^{2/\beta} \simeq (K_\mu t)^{2/\mu}, \tag{22}$$

we can see the superdiffusive character. In contrast, there are other strategies that make $\langle x^2(t) \rangle$ finite while retaining some properties of the power-law distributions. The most straightforward approach is to introduce a cut-off at the large value. Such distribution would have finite second moment and would thus in the limit of large number of jumps converge to Gaussian distribution with transient superdiffusive behavior. An alternative way that seems more physically justified is to penalize long jumps with long waiting periods, meaning that we couple $\psi(\tau)$ and $w(l)$ with respect to some finite velocity. Such process is the so-called Lévy walk [12].

4. Examples of Anomalous Diffusion

4.1 Subdiffusion of Molecules in Living Cells

4.1.1 Weak Ergodicity Breaking

Due to experimental difficulties or lack of suitable technology researchers were usually interested in ensemble-averaged quantities. However, with the development of single-molecule spectroscopy tracking of an individual molecules became possible. In contrast to ensemble averages, in single-molecule tracking one measures long trajectory of an individual particle in terms of time series $\mathbf{r}(\mathbf{t}')$ over a total trajectory duration T. Time-averaged MSD is then given by

$$\langle \mathbf{r}^2(t) \rangle_T = \frac{1}{T-t} \int_0^{T-t} \left[\mathbf{r}(t'+t) - \mathbf{r}(t') \right]^2 \mathrm{d}t', \qquad (23)$$

which integrates the squared displacement between the trajectory points separated by time lag t. In case of ordinary diffusion, equivalence $\langle \mathbf{r}^2(t) \rangle_T = \langle \mathbf{r}^2(t) \rangle_{\mathrm{ens}}$ holds for times $t \ll T$, provided that measurment time T is large compared to the time scale $\langle \tau \rangle$. This equivalence marks that a system is ergodic [5]. Since in subbdifusive CTRW heavy-tailed waiting time distributions (15) yield infinite $\langle \tau \rangle$, equivalence can not be reached, despite of a long measuring time. Therefore CTRW leads to weak ergodicity breaking. To compare theoretical CTRW model and experiment, double averaging is performed, which can be performed in desired order. Using ensemble-averaged MSD (16) we get a rough approximation:

$$\left\langle \langle \mathbf{r}^2(t) \rangle_{\mathrm{ens}} \right\rangle_T = \frac{1}{T-t} \int_0^T [\langle \mathbf{r}^2(t'+t) \rangle_{\mathrm{ens}} - \langle \mathbf{r}^2(t') \rangle_{\mathrm{ens}}] \mathrm{d}t' \approx \frac{AK_\alpha}{T-t} \int_0^T [(t+t')^\alpha - t'^\alpha] \mathrm{d}t', \qquad (24)$$

where A is some numerical prefactor. Assuming that $t \ll T$, we obtain

$$\left\langle \langle \mathbf{r}^2(t) \rangle_{\mathrm{ens}} \right\rangle_T \sim AK_\alpha \frac{t}{T^{1-\alpha}}. \qquad (25)$$

We see that such double average behaves as if diffusion was normal $\left\langle \langle \mathbf{r}^2(t) \rangle_{\mathrm{ens}} \right\rangle_T = AK_{\mathrm{eff}}t$ and that the effective diffusion coefficient depends explicitly on the averaging time T.

4.1.2 Experiment

Here we present an example of subdiffusive transport of a potassium channel protein in the membrane of human kidney cells reported by Weigel et al. [13]. They presumed that anomalous behavior is the consequence of transient immobilization of channel protein due to its binding to actin cytoskeleton. Such bindings result in long rests, which is typical of CTRW model. Experiment was done by using total internal reflection fluorescence microscopy that enabled tracking channel's position with nanometer accuracy. In order to compare time and ensemble averages they acquired 1015 trajectories, many of them longer than 10 min. They examined the time-ensemble-averaged MSD for all data at different lag times t. Figure 3(a) shows double averaged MSD against the measurement time T. For small T fluctuations can be observed, but for times T larger than 3 seconds MSD scales as power law $\langle \langle \mathbf{r}^2 \rangle_T \rangle_{\mathrm{ens}} \sim T^{\alpha-1}$ with $\alpha = 0.90 \pm 0.01$. Moreover, researchers were able to measure waiting time distribution by observing channel's immobilization. They identified the events in which the channel remained confined within a radius $R_{TH}^2 \ll$ MSD and constructed the distribution of waiting times from these events. Figure 3(b) displays waiting time distribution for three different radial thresholds. From the slope exponent $\alpha = 0.9$ can be identified, which corresponds to the value of measured MSD.

(a)   (b)
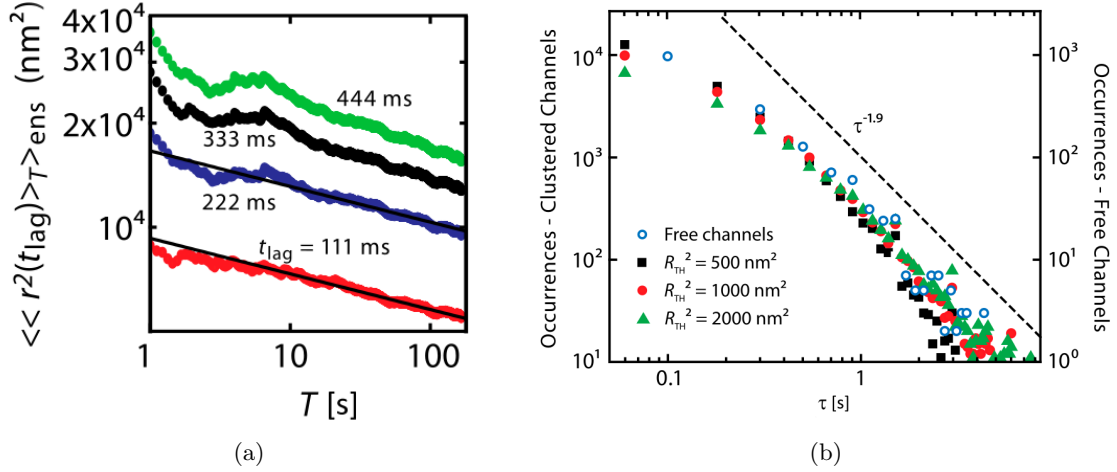
Slika 3. (a) Ensemble-time-averaged MSD of tracked channels for different lag times t. The MSD is plotted against the measurment time T used in the moving average. The straight lines show a power-law fit MSD$\sim T^{\alpha-1}$, with a slope $\alpha - 1 = -0.1$ (b) Measured distribution of waiting times using different radial thresholds. The dashed line indicates a power law $\psi(\tau) \sim 1/\tau^{-(1+\alpha)}$ with $\alpha = 0.9$. Reproduced from [13].

4.2 Superdiffusion in Monkey Behavior

In the study [14] of foraging patterns of free-ranging spider monkeys in the forest of the Yucatan Peninsula, Mexico, researches discovered that monkeys trajectories closely resemble CTRW. Both the distribution of waiting times between moves and distribution of continuous moves in the same direction could be approximated by previously introduced power-law functions, Eq. (15) and Eq. (20). Competition between long stops and long jumps [10] leads to MSD that scales as

$$\left\langle \mathbf{r}^2(t) \right\rangle \sim t^{2+\alpha-\mu}, \qquad 1 < \mu < 2, \quad 0 < \alpha < 1, \tag{26}$$

where α and μ correspond to exponents in waiting time (15) and step length (20) PDFs, respectively. Note that in the sections 3.1 and 3.2 we studied only the cases with either infinite waiting time or infinite second moment of step lengths distribution, while the other one being finite. Here, both PDFs are approximated by power-law and thus have infinite moments. The MSD (26) is therefore a result of a more complicated theory that takes into account both effects, see [5] and [10].

Data were collected in the area of the forest surrounding the Punta Laguna lake, between September through December 1999. On 20 days during this period, a different adult monkey was chosen as a focal point and was followed by at least two observers from dusk to dawn, taking an instantaneous sample of its location every 5 minutes. The location was estimated with respect to previously established map that used special landmarks, trees and trails. The trajectory of each monkey consisted of paired coordinates, one for each 5 min interval where a sample had been recorded. A step was defined as an interval in which any or both of the successive coordinates changed. The length of each step was the linear distance between two consecutive positions. To analyze the distribution of the step lengths bin size of 10 m was used. Then the data were log-log transformed and the best fit was evaluated using a least-square method, see Fig. 4(a). Waiting times were obtained from the number of samples in which the focal animal did not change position. The waiting time distribution was then analyzed using a bin size of 5 min and then log-log transformed to produce the best fit using least-square method, see Fig. 4(b). The mean squared displacement $\langle \mathbf{r}^2(t) \rangle$ was calculated in the following manner: first, the length of the line connecting the first recorded location of each individual with its location at different times thereafter was measured. Then, all individual squared displacements were averaged for each time of day. Researches considered only
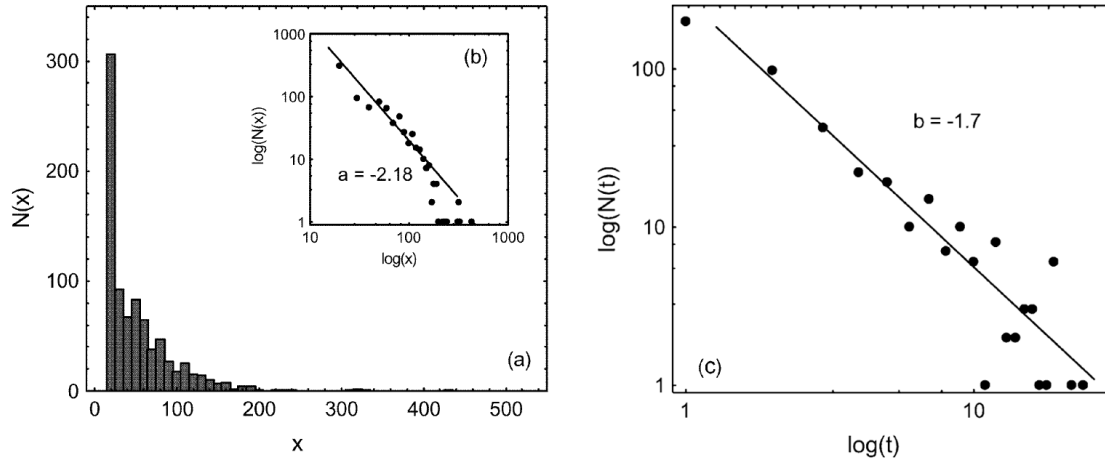
Slika 4. (a) Distribution of the number of 5 min intervals $N(x)$ during which spider monkeys traveled a distance of x m. A total of 841 5 min intervals from 20 adult individuals are included. Inset (b) displays log-log transformed data $N(x)$ that is fitted with power-law relationship, $N(x) \propto x^a$. The estimated value of the exponent is -2.18. (c) Log-log plot of distribution of waiting times (intervals $N(t)$ with duration t). The relationship is fitted by a power-law function, $N(t) \propto t^b$, with an estimated value of the exponent of -1.7. Reproduced from [14].

the MSD between 6:30 and 10:30 am. After this period the MSD decreased as the animals started to approach their starting point, see Fig. 5(a). From Figs. 4 and 5 we see that the log-log plot of the
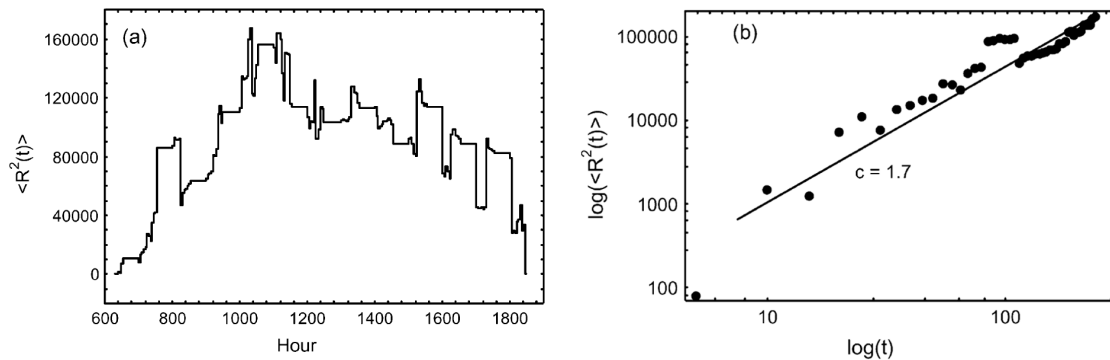
Slika 5. (a) MSD across all individual trajectories at different times of day with a maximum at 1030 hours. (b) Log-log transformation of the MSD observed from 0630 to 1030 hours. Transformed MSD is well fitted by a power-law function, $\langle R^2(t) \rangle \propto t^c$, with an estimated value for the exponent of 1.7. Reproduced from [14].

data is fitted well by a negative power-law function in both distributions. By comparing functions used for fitting in Fig. 4 with waiting time PDF (15) and jump length PDF (20) we observe that the relations between fitting parameters b, a and α, μ go as $\alpha = -b - 1$, $\mu = -a - 1$. Using Eq. (26) we can now predict the value of c

$$c = 2 + \alpha - \mu = 2 - b + a = 1.52, \tag{27}$$

which is quite close to the observed value 1.7 in Fig. (5)(b). To sum up, with this study researches showed that the step lengths distribution and the distribution of waiting times between steps behave as power-law functions. Moreover, the theoretical model (26) was shown to be rather accurate in predicting MSD scaling with time.

5. Conclusion

Anomalous diffusion can be observed in numerous systems from various disciplines including physics, chemistry, engineering, geology, biology, economy, meteorology, astrophysics and others. However, there is no universal physical and mathematical model to describe such processes. Due to many different physical mechanisms there are many models to describe anomalous diffusion, see [9]. In this article we focused on CTRW that can be successfully used to model systems where long waiting times or long jumps occur.

6. Acknowledgement

LITERATURA

[1] Scher, H. & Montroll, E. W. Anomalous transit-time dispersion in amorphous solids. *Physical Review B* **12**, 2455–2477 (1975).

[2] Viswanathan, G. M. et al. Lévy flight search patterns of wandering albatrosses. *Nature* **381**, 413–415 (1996).

[3] Klafter, J. & Sokolov, I. M. Anomalous diffusion spreads its wings. *Physics World* **18**, 29–32 (2005).

[4] Metzler, R. & Klafter, J. The restaurant at the end of the random walk: recent developments in the description of anomalous transport by fractional dynamics. *Journal of Physics A: Mathematical and General* **37**, (2004).

[5] Sokolov, I. M. & Klafter, J. M. *First Steps in Random Walks: From Tools to Applications.* (Oxford University Press, 2011).

[6] Weiss, G. H. *Aspects and applications of the random walk.* (North-Holland, 1994).

[7] Sokolov, I. M. Models of anomalous diffusion in crowded environments. *Soft Matter* **8**, 9043 (2012).

[8] Metzler, R., Jeon, J.-H., Cherstvy, A. G. & Barkai, E. Anomalous diffusion models and their properties: non-stationarity, non-ergodicity, and ageing at the centenary of single particle tracking. *Phys. Chem. Chem. Phys.* **16**, 24128–24164 (2014).

[9] Klages, R., Radons Günter & Sokolov, I. M. *Anomalous transport: foundations and applications.* (Wiley-VCH, 2008).

[10] Metzler, R. & Klafter, J. The random walks guide to anomalous diffusion: a fractional dynamics approach. *Physics Reports* **339**, 1–77 (2000).

[11] Širca, S. *Probability for Physicists.* (Springer International Publishing, 2016).

[12] Zaburdaev, V., Denisov, S. & Klafter, J. Lévy walks. *Reviews of Modern Physics* **87**, 483–530 (2015).

[13] Weigel, A. V., Simon, B., Tamkun, M. M. & Krapf, D. Ergodic and nonergodic processes coexist in the plasma membrane as observed by single-molecule tracking. *Proceedings of the National Academy of Sciences* **108**, 6438–6443 (2011).

[14] Ayala-Orozco, B. R. et al. Lévy walk patterns in the foraging movements of spider monkeys (Ateles geoffroyi). *Behavioral Ecology and Sociobiology* **55**, 223–230 (2004).